Fire resistant and mechanical properties of bagasse packaging paper coated with hexachlorocyclodiphosph(V)azane/starch/NaHCO₃/ CaCO₃/cellulose nanocrystals composite ☆

A.A. Younis [a,*], S.A.A. Mohamed [b], M. El-Sakhawy [c]

[a] Gas Analysis and Fire Safety Lab, National Institute of Standards, Tersa St, El-Matbaa, Haram, P. O. Box: 136, Code No. 12211 Giza, Egypt
[b] Packaging Materials Department, National Research Centre, 33 El-Bohouth St., [former El Tahrir st.], Dokki, P.O. 12622, Giza, Egypt
[c] Cellulose and Paper Department, National Research Centre, 33 El Bohouth St. [former El Tahrir st.], Dokki, P.O. 12622, Giza, Egypt

ARTICLE INFO

ABSTRACT

This work aimed to enhance the thermal and mechanical properties of bagasse paper by synthesizing new coatings to prevent bagasse paper from the ignition. Paper sheets were treated with 0.5 percent cychlodiphosph(V)azane/ CaCO₃ solution (1.5 percent), 1.5 percent NaHCO₃ solution, and CNCs mixed with 5.0percent of starch. Paper sheets were treated by immersing bagasse paper in a coating mixture. The paper sheets were then allowed to air dry at ambient temperature. It is important to measure the burning rate (BR) to give people a chance to decrease the loss. These enhancements were investigated using elongation and tensile strength, air permeability test, Fourier Transform Infrared (FTIR) spectroscopy, thermal gravimetric analysis (TGA), and combustion tests (UL/94 and LOI). So, the bagasse paper treatments can be used as packaging materials.

1. Introduction

The most common material used to lower composite production costs and increase thermal characteristics is sodium bicarbonate(NaHCO₃) [1]. The effect of NaHCO₃ as a fire retardant addition during combustion or pyrolysis is explored in various researches. According to pyrolysis data, adding NaHCO₃ causes a shift toward lower degradation temperatures for the studied species. As a result, NaHCO₃ lowers the initial temperature of pyrolysis in the studied species. Otherwise, NaHCO₃ increases the time it takes for forest species to self-ignite and the length of time it takes to burn (inhibition effect). Furthermore, NaHCO₃ increases the pyrolysis mass residue of forest species [2].

Also, the mechanical, thermal, and ignition capabilities of bagasse paper is improved by coatingwith hydroxyethyl cellulose, 1,3-di-p-Aryl-2,2,2,4,4,4-hexachlorocyclodiphosph(V)azane, Talc powder, NaHCO₃, and cellulose nanocrystal was recorded. The bagasse paper sheets properties of were improved in this work

using a simple and low-cost process involving the creation of new coatings using commercially available chemicals at a sensible cost [3].

Prepared ethylene–vinyl acetate (EVA)composites using CaCO₃-containing oil sludge (OS) and carbon black (CB), were discovered. It was found that adding CaCO₃-containing OS and CB improved the thermal stability and flame retardancy of composites [4]. A new method for CaCO₃ deposition in wood has been proposed, boosting carbon dioxide content and fire resistance. The approach involved vacuum impregnation of wood with aqueous calcium chloride solution and successive sequential diffusion of gaseous ammonium and carbon dioxide to enhance the mineralization of radiata pine wood microstructure with CaCO₃. The approach produced a weight gain of around 20% due to mineralization in the most favorable conditions, implying the buildup of 0.467 mmol g^{-1} carbon dioxide in the microstructure of wood. Furthermore, an 8 percent weight gain was adequate to offer fire resistance comparable to a commercially available fire-retardant therapy. It may be useful to manufacture wood products with improved environmental qualities if carbon dioxide can be retained directly inside the wood microstructure. This strategy could be a viable option for people looking for resources to help them achieve a fully sustainable development [5].

When starch is mixed with fibre and filler [6], it forms a soft gel layer between fiber–fiber connections on the surface of both filler and fibre, increasing the paper's tensile index and stiffness. The mechanical characteristics of paper containing talc increased by 61.9 percent by combining it with starch (cooked talc –starch) [7]. Neutral starch retention in a pulp furnish is less than 40% [8]. Because pulp furnishes are negatively charged, starches are frequently changed as cationic charged or amphoteric starches to enhance starch retention [9]. Cationic starch increased the Scott bond, tensile strength, and burst index [10]. The cost of starch is frequently increased due to the starch modification process. The findings show that altering starch and bagasse for tissue paper improves mechanical and absorbency qualities. This was owing to the establishment of large pore size in the fibres, which can aid in water absorption, and to the link formed between the modified starch and the fibres during the papermaking process [11].

This work aimed to enhance the mechanical, thermal, and ignition properties of bagasse paper by synthesizing new coatings. These enhancements were investigated using elongation and tensile strength, air permeability test, Fourier Transform Infrared (FTIR) spectroscopy, thermal gravimetric analysis (TGA), and combustion tests (UL/94 and LOI). Starch was employed to increase the qualities of the paper sheets, improve the mechanical properties, and to homogenize the used coating formulations. Cychlodiphosph(V)azanewith its obvious flame retardant characteristics was prepared from the commercial phosphorus pentachloride and p-chloroaniline or aniline and employed in a coating mixture. Furthermore, CaCO$_3$ and NaHCO$_3$ werea commonreadily available low-cost filler mostly usedto lower composite production costs and improve thermal characteristics. Besides, the addition of nanocellulose to nanocomposites has significantly improved their thermal and mechanical properties.

2. Experimental

2.1. Material and methods

A sheet of blended bagasse paper with a basis weight of 80 g/m^2 was purchased from Rakta Company, Egypt. It was applied as a blank specimen. Both CaCO$_3$ and NaHCO$_3$ were purchased as powders from El-Gomhouria Company in Egypt. In contrast, the starch and sulphuric acid (99.9%, ADWIC) were purchased from Netherlands and Germany, respectively. The usually used solvent was tap water.

2.2. Synthesis of cellulose nanocrystals (CNCs)

Sulphuric acid was used to treat bleached bagasse pulp with vigorous stirring for 45 min. The process was achieved at 45 °C. After the reaction was stopped by adding ice to the solution, the mixture was centrifuged and sonicated for 15 minutesin an ice bath [12].

2.3. Synthesis of 1,3-di-Aryl-2,2,2,4,4,4-hexachlorocyclodiphosph(V) azane

The Chapman techniques [13] were used to make 1,3-di-aryl-2,2,2,4,4,4-hexachlorocyclodiphosph(V)azane, in which cold dry benzene phosphorus pentachloride interacted with aryl (aniline or p-chloroaniline) to provide 1,3-di-aryl-2,2,2,4,4,4-hexachlorocy clodiphosph(V)azane. Secondly, in a round flask attached to the condenser, 0.1 mol aniline dissolved in 100 ml benzene was added dropwise to PCl$_5$ (20.9 g, in 200 ml benzene) in a round flask with stirring for 1 h at 15 °C, then heating at 250 °C for 3 h by the heating mantle. By cooling the mixture to ambient temperature, filter-

ing, and washing the solid crystal multiple times with dry ice, the hexachlorocyclodiphosph(V)azane was eventually produced as solid crystals [14] (Fig. 1).

2.4. Coating the paper specimens using nanocomposite

Table 1 illustrates thatthe bagasse paper sheets were treated with 0.5% cychlodiphosph(V)azane, 1.5% CaCO$_3$, 1.5% of NaHCO$_3$ solution, and cellulose nanocrystals (CNCs) which were mixed with different concentration of starch as illustrated inTable 1. The treatment of paper sheets was performed by coating bagasse paper in a coating mixture for 30sec, and then the excess solution was removed by filter paper. The paper sheets were then allowed to air dry at ambient temperature.

2.5. Characterization of papers

After coating with a gold/palladium alloy, the morphology of the specimens was observed using a scanning electron microscope (SEM, a Zeiss ULTRA55) with an accelerator voltage of 15 kV. A sputter coater system (Edwards Sputter Coater; BOC Edwards, Sussex) was used to apply the coating.

The specimens' infrared spectra were collected using a Nicolet 380 Spectrometer and Fourier Transform Infrared (FTIR) Spectroscopy (USA). This test aimed to see how the functional groups of the untreated and coated specimens changed. The spectra were taken at wavenumbers ranging from 4000 to 500 cm^{-1} [15]. The absorbent frequencies were 32 scans with a resolution of 4 cm^{-1} and a pressure of 18 Kpa.

2.6. Mechanical and barrier properties

Films used in food packaging must have a high level of air permeability. The oxygen is a crucial component that can permeate packaging materials and impair the quality of food. Bendtsen smoothness and porosity tester produced in Denmark, Andersson Sorensen, Copenhagen, was used to determine the air permeability of the films. The rate of airflow between the film's surface and two metal rings affixed to the film was measured under standard pressure to assess air permeability [12]. The thickness of the specimens was measured using a hand-held micrometer, with an average of five measurements taken. According to ISO 2758 [16], the burst strength was used to determine specimens resistance to exploding. Universal testing equipment was used to measure the elongation and tensile strength of the samples at room temperature (LR10K; Lloyd Instruments, Fareham, UK). The gap between the jaws is 10 mm, and the crosshead speed is 0.6 mm/min for 250 sec, then 1.5 mm/min for 2000 sec, and ultimately 3 mm/min till the break. The specimen was 20 × 5 mm^2 in size [17].

2.7. Thermal characteristic

Thermal Gravimetric Analysis (TGA) is used in conjunction with endnote and ash residue at various phases of specimen deterioration. This test was carried out using an SDT Q600 V20.9 Build 20 Instrument (USA) [18]. The experiment was conducted in a nitrogen environment at a 30 ml/min flow rate, a heating rate of 10 °C/min [19], and a temperature range of 30–1000 °C [20].

2.8. Flame retardantmeasurement

The effect of the new coating was evaluated by:
1. The 45-degree flammability test
This test calculates the ignition time of the specimen by hanging the specimen at 45°and exposed to a horizontal butane gas burner with a flame length of 6.5 cm for 1sec, then removing the
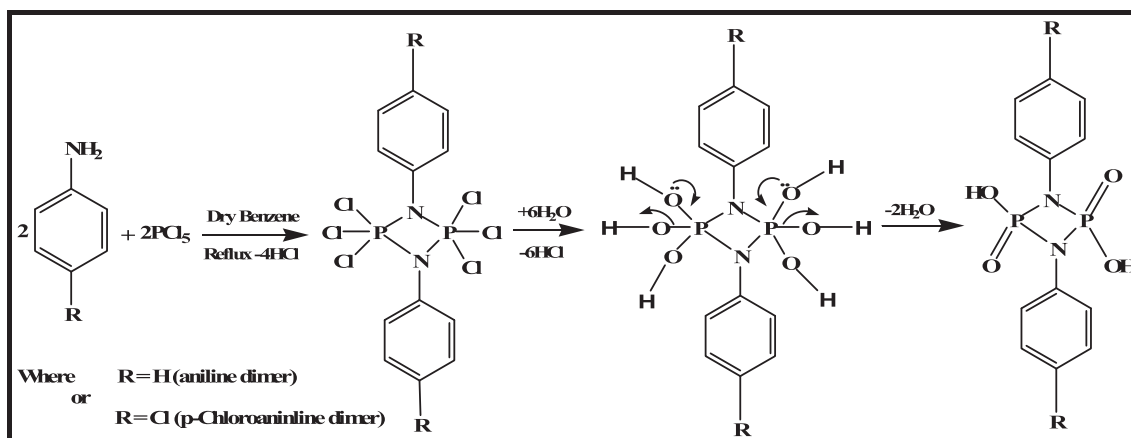
Fig. 1. The chemical reaction to synthesis hexachlorocylodiphosphazanederivatives.

Table 1
Coating composition for paper sheets.

Codes	Starch %	NaHCO$_3$ %	CaCO$_3$ %	Aniline dimer %	p-chloroaniline dimer %	CNC %
SK0	—————	—————	—————	—————	—————	————
SK1	3.50	—————	—————	—————	—————	————
SK2	3.50	—————	—————	—————	0.50	————
SK3	3.50	—————	—————	0.50	—————	————
SK4	5.00	—————	—————	—————	—————	———
SK5	5.00	1.50	1.50	—————	—————	————
SK6	5.00	1.50	1.50	0.50	—————	————
SK7	5.00	1.50	1.50	—————	0.50	————
SK8	5.00	1.50	1.50	0.50	—————	10
SK9	5.00	1.50	1.50	—————	0.50	10

burner and calculating the total time of burning test specimen. This test is performed at ambient temperature.

2. Char length measurement

The char length was measured according to BS 3119 standard [21].

3. Flammability test

It was important to measure the burning rate (BR) [22] to give people a chance to escape. Firstly, the specimens were cut in the dimensions of 5 cm × 15 cm with a thickness of 0.1 cm, held horizontal before exposing to 2 cm of the burner(propane gas) with an angle of 45° [23,24]. After 2sec from directly exposed to the burner in Stanton-Redcroft (made in UK), the length and time of burning were recordedafter the flame passed the first line (after 2.5 cm from the free edge). The BR was calculated by the equation (1) [25]:

$$Burn\ Rate(BR) = 60 \times [Burning\ Distance/Burning\ Time][mm/min] \tag{1}$$

2.9. Flame retardant behavior

The behavior of ignition was studied. Firstly, the test specimens were dried at ambient temperature for 48 h before use, then cut the specimens in dimensions 5 × 15 cm^2. The U frame was used to hang the test specimen before holding it vertically. A burner with a length of 2 cm was used to ignite the top free edge for 15sec [26].

2.10. Oxygen index

This test determine the low concentration of oxygen needed to ignite the specimen for 3 min. According to the standard method, this test was achieved using a Rheometric Scientific instrument

[27]. The specimens were cut in 5 cm in width and 15 cm in height before hanging vertically in the U holder [28]. A mixture of oxygen and nitrogen gases was used since the oxygen gas was a fuel source, while nitrogen gas aimed to isolate the test specimen from other gases. The propane gas was used for 30sec [29] as a burner, then removed and noticed the combustion behavior of the test specimen. At ambient temperature, the average values of LOI % for five replicates were taken [30].

3. Results and discussion

The bagasse paper sheets were treated with 0.5% cychlodi-phosph(V)azane/ 1.5% CaCO$_3$, 1.5% NaHCO$_3$ solution, and CNCs mixed with different concentration of starch (Table 2). Paper sheets were treated by coating bagasse paper in a coating mixture. The paper sheets were then allowed to air dry at ambient temperature. Untreated and treated specimens had average thicknesses of 0.113 to 0.232 mm.

^{1}H NMR spectra of for 1,3-di-p-aryl-2,2,2,4,4,4-hexachlorocyclo diphosph(V)azane

Figs. 2 and 3 show the^{1}H NMR spectrum of p-chloroaniline and aniline dimers, respectively. Due to the resonance of the different types of aromatic protons, a multiplet occurs in the range of 7.2–8.6 ppm and 6.9–8.6 ppm for p-chloroaniline and aniline dimers, respectively. The broad signal, which appears in the range of 10.3–11.3 ppm, is due to the proton of the NH group which may be formed from the resonance between delocalization of the lone pair on P-N and the protons on benzene rings. Finally, the sharp singlet signal at 2.4 ppm corresponds to the absorption of protons in the DMSO- CH$_3$ group.

Table 2

Mechanical properties and air permeability for paper sheets.

Codes	Maximum load (N)	Percentage strain at maximum load	Young's modulus (MPa)	Burst	Air permeability s/100 cm³
SK0	16.83 ± 0.92	2.89 ± 0.12	0.0818 ± 0.24	0.95 ± 0.39	54.0 ± 2.74
SK1	25.85 ± 1.21 (53.59)	2.29 ± 0.23	0.1044 ± 0.18 (27.63)	1.1 ± 0.33 (15.79)	620.0 ± 0.41 (1048.15)
SK2	20.48 ± 3.54 (21.69)	1.002 ± 1.62	0.423 ± 0.16 (417.58)	1.2 ± 0.14 (26.32)	201.0 ± 3.70 (272.22)
SK3	18.58 ± 1.37 (10.40)	5.882 ± 0.29	0.487 ± 0.04 (496.30)	1.2 ± 0.11 (26.32)	2095.8 ± 5.68 (3781.11)
SK4	32.85 ± 2.32 (95.19)	3.39 ± 0.28	0.1224 ± 0.013 (49.63)	1.3 ± 0.13 (36.84)	1140.0 ± 4.07 (2011.11)
SK5	20.63 ± 0.66 (22.58)	2.43 ± 0.34	0.1157 ± 0.0081 (41.44)	1.2 ± 0.51 (26.2)	11040.0 ± 1.72 (20344.44)
SK6	21.88 ± 1.53 (30.01)	2.90 ± 0.30	0.1213 ± 0.0152 (48.29)	1.35 ± 0.31 (42.11)	7968.0 ± 3.48 (14655.56)
SK7	22.04 ± 1.76 (30.96)	3.15 ± 0.24	0.1312 ± 0.0156 (60.39)	1.1 ± 0.32 (15.79)	2264.0 ± 8.81 (4092.59)
SK8	22.74 ± 0.74 (35.12)	2.81 ± 0.18	0.1364 ± 0.0197 (66.75)	1.1 ± 0.08 (15.79)	5520.0 ± 18.97 (10122.22)
SK9	22.30 ± 1.77 (32.50)	2.77 ± 0.03	0.1309 ± 0.0203 (60.02)	1.05 ± 0.13 (10.53)	2592.0 ± 15.22 (4700.00)

The numbers in brackets refer to the increasing percentage compared with the untreated sample.
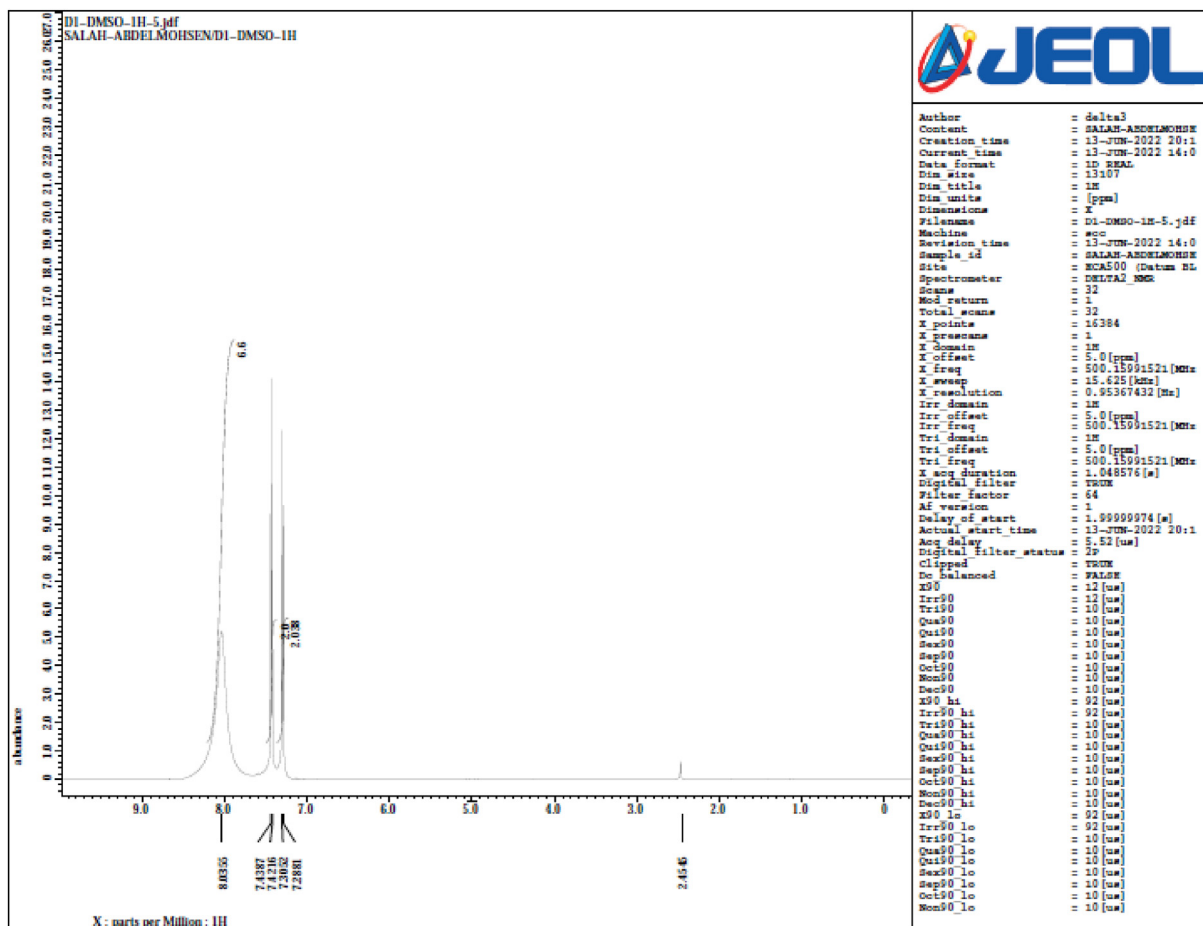
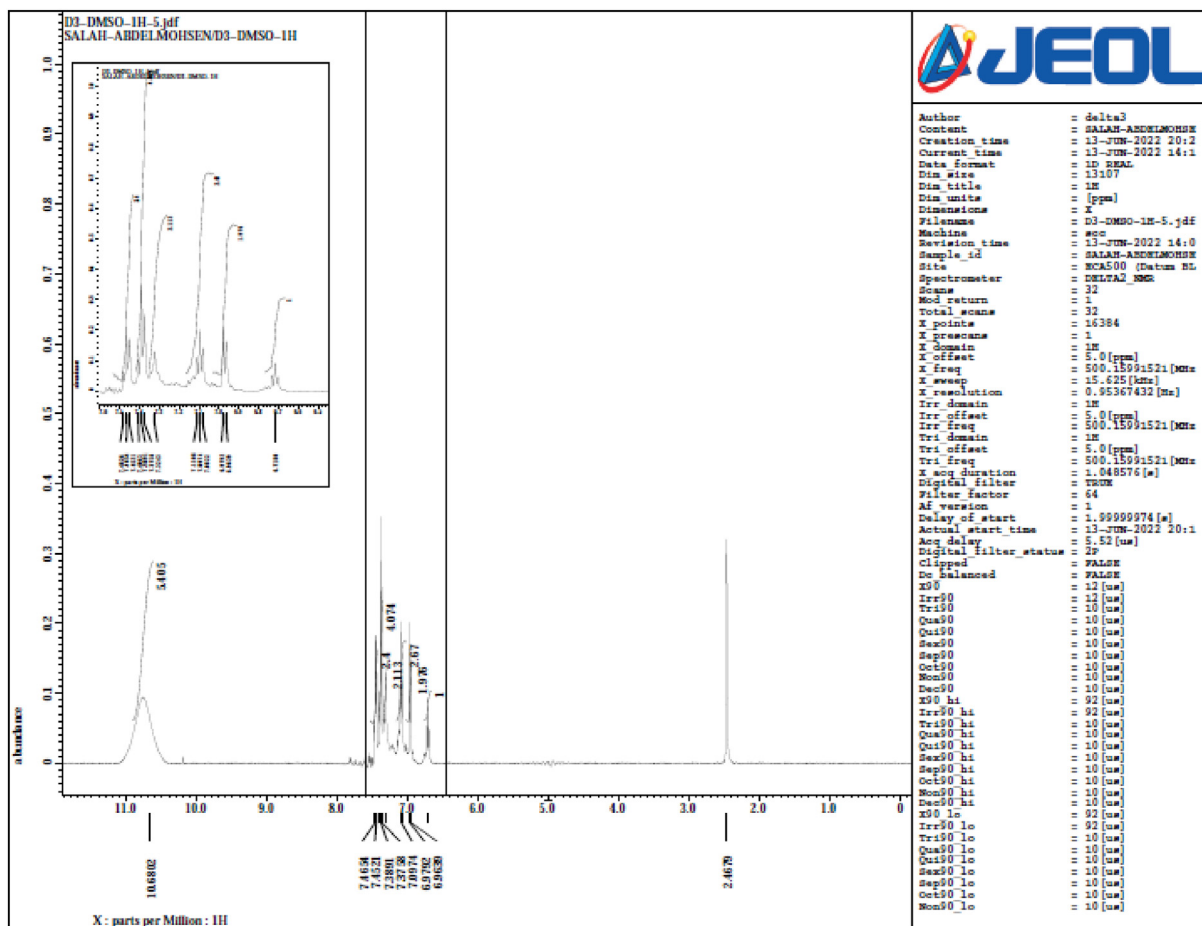**Fig. 2.** ^{1}H NMR spectrum for 1,3-di-p-chloroaniline-2,2,2,4,4,4-hexachlorocyclodiphosph(V)azane in DMSO ^{1}H.

Fig. 3. ^{1}H NMR spectrum for 1,3-di-aniline-2,2,2,4,4,4-hexachlorocyclodiphosph(V)azanein DMSO ^{1}H.

3.1. X-Ray diffraction and transmission electron microscopy (TEM) (XRD)

TEM and XRD were used to characterise the morphological structure of cellulose nanocrystals, which described the rod-like CNCs formed. Fig. 4 exhibits nanocrystal aggregates. Because of the high specific area and strong hydrogen bonds formed between the CNCs, aggregated elementary crystallites should appear in TEM images. The presence of two peaks at 2θ 18° and 22° was shown by the XRD test and the size of cellulose nanocrystals was calculated in our previous works [12].

3.2. Mechanical properties of paper sheets

3.2.1. Tensile Strength(Maximum Load (N))

Table 2 shows the results of coating paper sheets with 0.5 percent aniline dimer or p-chloroaniline dimer in the presence of 10% CNCs and other additives. The significant factor impacting the tensile strength of paper sheets is the amount and quality of fibre bonding. The tensile strength (TS) of paper sheets was enhanced by (53,95%) when treated with 3.5% starch (SK1). On the other hand, it improved by 21.7 and 10.4% after adding p-chloroanilinedimer or aniline dimer,respectively to 3.5% starch. The addition of 1.5% NaHCO$_3$ and 1.5% CaCO$_3$ to 5.0% starch increased TS by 22.5%. Adding 0.5% p-chloroaniline dimer or aniline dimer to them as in SK6, SK7 specimens the TS increased by 30.9–30.0%, respectively.

Furthermore, adding CNCs (10%) enhanced TS by 32–35 percent. Because of its nano-sized diameter and significantly bigger surface area than pulp fibres, the presence of aniline dimer and CNCs with pulp fibres results in increased hydrogen bonding between them. The achieved improvement is due to improved interaction between the OH groups of cellulose and the accessible groups of aniline or p-chloroaniline dimers and CNCs. The addition of starch and the presence of aniline or p-chloroaniline dimers affect the elongation of paper sheets besides the tensile strength by 103.5, 17.3, and 9.00% after addition of starch/aniline dimer, starch only, and starch/NaHCO$_3$/CaCO$_3$/p-chloroaniline as in SK3, SK4, and SK7 specimens, respectivly.

3.3. Young's modulus

Young's modulus measures a specimen's stiffness; it linearly connects stress and strain. Young's modulus rose because the samples' density was more than the blank (due to the filler addition). It was enhanced by around (27–496%) compared to the blank.

3.4. Burst strength

The impact of aniline or p-chloroaniline dimers, 1.5% NaHCO$_3$ and 1.5% CaCO$_3$ to 3.5% starch and 10% CNCs, on the burst strength of bagasse pulp paper sheets was investigated. Fiber length, inter-fiber bonding, and sheet stretch influence burst strength [31]. The burst strength follows the same pattern as the breaking length, with stronger burst strength (10–42% higher) than those manufactured from bagasse fibres. The presence of starch and CNCs, improved the mechanical characteristics.
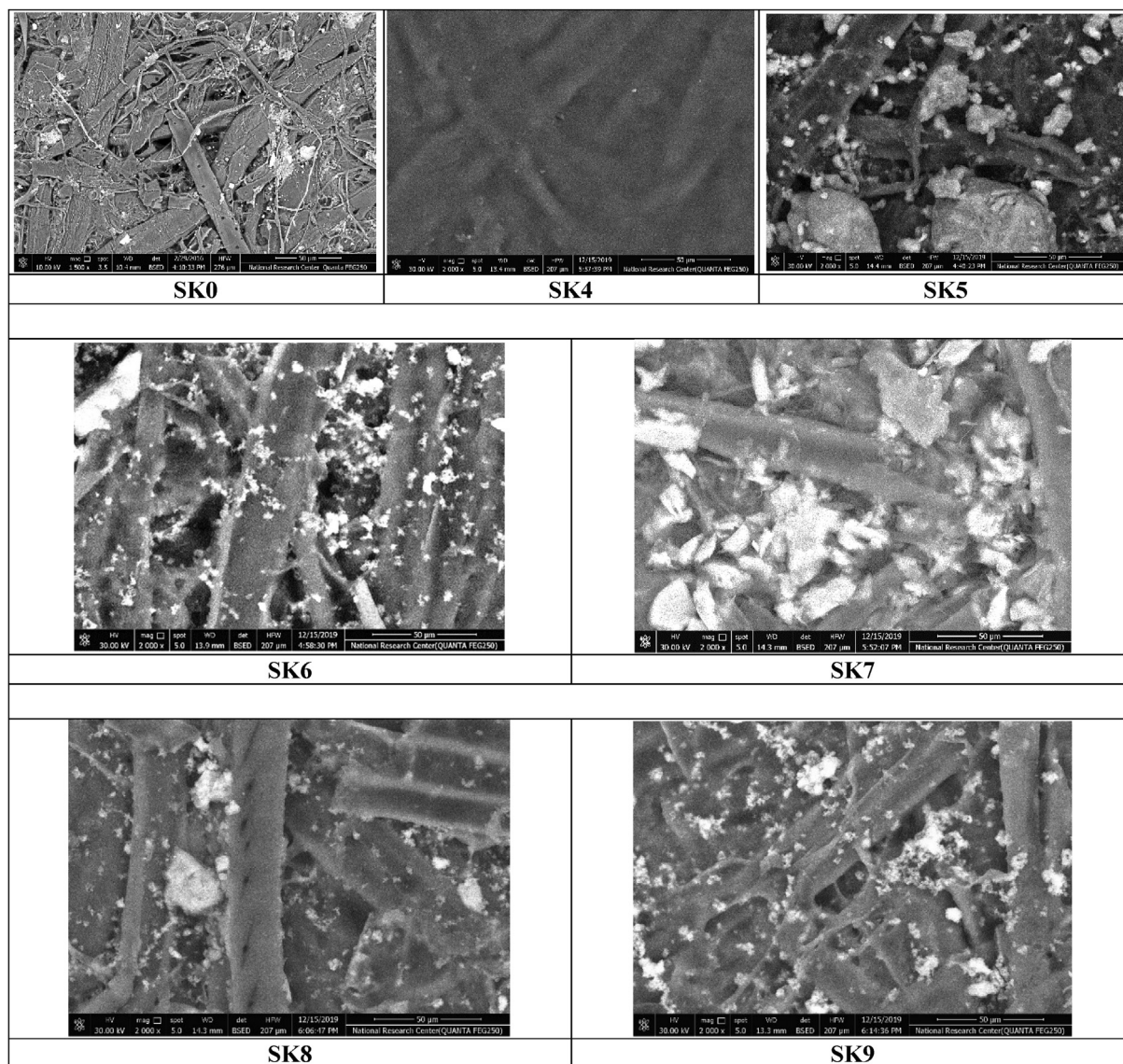
Fig. 4. SEM micrographs of; SK0: Untreated bagasse paper, SK4: Specimen coated with 5.0% starch only, SK5: Specimen coated with 5.0% starch/1.50%NaHCO$_3$/1.50%CaCO$_3$, SK6: Specimen coated with 5.0% starch/1.50%NaHCO$_3$/1.50%CaCO$_3$/0.50% aniline dimer, SK8: Specimen coated with 5.0% starch/1.50%NaHCO$_3$/1.50%CaCO$_3$/0.50% aniline dimer/10% CNCs, SK9: Specimen coated with 5.0% starch/1.50%NaHCO$_3$/1.50%CaCO$_3$/0.50% p-chloroaniline dimer /10% CNCs.

3.5. Physical properties of paper sheets

Apart from improving the mechanical qualities of paper sheets like tensile and burst strength, aniline or p-chloroaniline dimers, 1.5% NaHCO$_3$ and 1.5% CaCO$_3$ to (3.5%) starch, and 10% CNC scan also contribute to other functional aspects, as illustrated in Table 2. Reduced air permeability is one of these functional qualities. Compared to the blank, all samples demonstrated lower air permeability after coating. These decreases were 1048, 272, 3781, 2011, 20344, 14655, 4092, 10122, and 4700% in SK1, SK2, SK3, SK4, SK5, SK6, SK7, SK8, and SK9, respectively. These can show that adding aniline or p-chloroaniline dimers, 1.5% NaHCO$_3$ and 1.5% CaCO$_3$ to (3.5%) starch and 10% CNCs gave superior enhancement to the surface of the blended bagasse paper sheets. The barrier to air movement increases when coating compounds fill the paper sheets pores. This could be because the additives have penetrated the cellulose matrix. The nano-sized diameter and the superior surface area of aniline dimer and CNCs than pulp fibres results in increased hydrogen bonding between them. In addition, various functional groups in aniline dimers and CNCs improved the interaction between the cellulose OH groups and the accessible groups of aniline or p-chloroaniline dimers and CNCs.

3.6. Scanning electron microscope (SEM)

A scanning electron microscope was used to image the blank and coated bagasse paper sheets. Fig. 4 shows that the paper sheets with coating ingredients had a substantially denser surface structure than the blank (K0). As illustrated in Fig. 4, the K0 surface has numerous pores of various sizes, responsible for quickly shredding of the paper sheet through the mechanical test.

For K4 sample, adding 5% of starch shows a smooth surface as starch filled the pores and covered the surface with a coated thin layer which decreases the air permeability. The air permeability decreased by increasing the aniline dimer or p-chloroaniline dimers, 1.5% NaHCO$_3$ and 1.5% CaCO$_3$ to (3.5%) starch and 10% CNCs. The lowest percentages of air permeability have been found in K5, SK6, and SK8, which appeared in the Scanning Electron Microscope with excellent coating distribution on the paper sheet surface. SEM shows that all additives were added invery good

ways. It may produce an interchemical reaction, as evidenced by theexcellent molecular distribution of the reactants.According to the results, some additives may produce a film over the sheet after coating, these films over the sheet decrease the air permeability because they filled the pores and cover the surface by a coated thin layer.

3.7. FT-IR spectra

Fig. 5 shows FTIR for the various specimens. The FTIR spectra of blank (blended bagasse paper sheet) (K0) show broad bands at 3400 cm^{-1}, which can be assigned to the OH in cellulose. In SK4 the broad bands at 3400 cm^{-1} became strong because the addition of starch may increase the OH groups. However, it is well understood that the infrared spectrum is usually congested with bands that overlap between cellulose and starch. But increasing in the broad bands at 3400 cm^{-1} could confirm that starch was loaded

sucessfuly on the surface of cellulose of the paper sheets but there are overlapping of cellulose and starch peaks. In SK5, SK8, and SK9 these broad band decreased, may be according to the reactions between NaHCO$_3$ and CaCO$_3$ with OH groups in the surface of cellulose after addition of starchthat almost disappears in SK9. By the addition of NaHCO$_3$ and CaCO$_3$, aniline dimer or p-chloroaniline dimer a reacteion with OH groups on the surface of paper sheets occurs and resulted in the decreasing of the broad band at 3400 cm^{-1} until it disappeared finaly in SK9. The observation of the signals of these vibrations further indicated that OH groups of cellulose and starch were deprotonated. These results suggest that the OH groups of cellulose and starch interacted or coordinated with Ca^{2+}, Na$^+$, or P^{3+} ions via bridge coordination or chemical reactions. The spectra of (SK8 and SK9) show a new strong, broad band at 1655 cm^{-1}, which can be assigned to the P-O symmetrical deformation, which refer to the reaction between P-N-P in aniline or p-chloroaniline dimers and OH groups on the surface
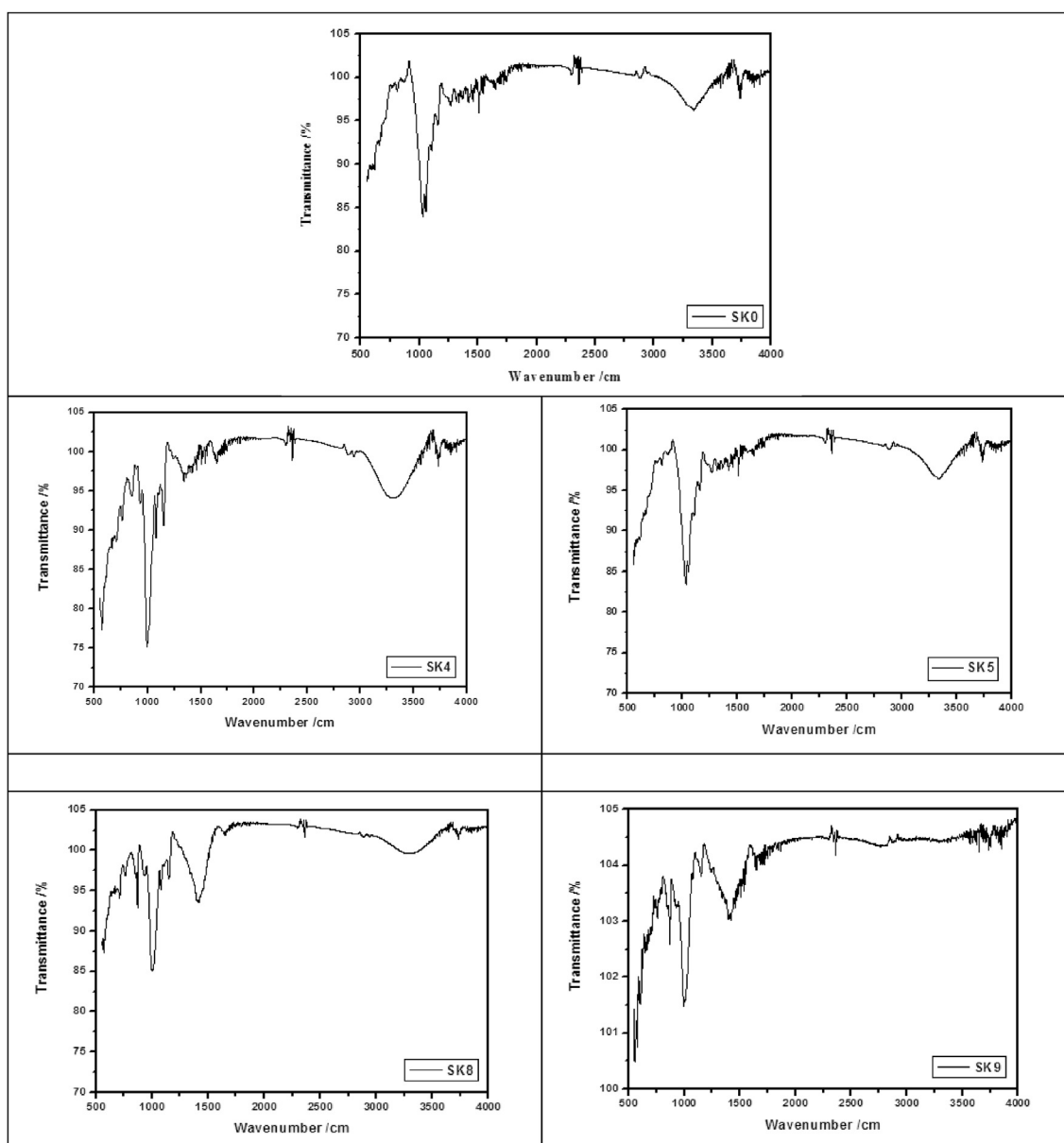

Fig. 5. FTIR Spectrum of SK0: Untreated bagasse paper, SK4: Specimen coated with 5.0% starch only, SK5: Specimen coated with 5.0% starch/1.50%NaHCO$_3$/1.50%CaCO$_3$, SK8: Specimen coated with 5.0% starch/1.50%NaHCO$_3$/1.50%CaCO$_3$/0.50% aniline dimer/10% CNCs, SK9: Specimen coated with 5.0% starch/1.50%NaHCO$_3$/1.50%CaCO$_3$/0.50% p-chloroaniline dimer /10% CNCs.

of cellulose. It illustrates the P-N groups' stretching vibration bands in the 1453–1381 cm^{-1} range. At 1156–1162 cm^{-1}, cellulose exhibits asymmetrical stretching (C-O-C). The C-O band in cellulose and starch is given to the sharp peaks at 1066 and 1035 cm^{-1}, that other overlap between cellulose and starch, but it was higher for the SK4 sample. At 888 cm^{-1}, the connections between glucose units (b- glycosidic) emerged. The peak shows the existence of (C-OH) out of plane bending of cellulose at 670 cm^{-1}.

3.8. Thermal analysis

The degradation stages and residual ash percentage of every specimens are illustrated in Fig. 6. In the Fig. 6a, the water evaporated in the first stage of SK0 specimen degradation up to 100 °C, then the presence of CO and CO$_2$ gases with high percentages in between 100 and 330 °C due to analysis of glucose, galactose, and mannose which produced from hemicellulose in the second stage. Finally stage of degradation located up to 1000 °C, where completely decomposes of cellulose (with loss of weight 30%) [32], and lignin (aromatic rings) [33]. The stability and ash residue are enhanced by increasing the starch percentage from 3.5% to 5.0%. The stability of SK4 specimen after evaporating water (up to 110 °C) improved up to 248 °C, and ash residue percentage increased from 1.3% in case of SK0 specimen up to 18.0% then

raised by rise the percentage of starch to record the highest percentage of ash residue (24.8%) in case of SK4 specimen. The effect of NaHCO$_3$ and CaCO$_3$ on reducing heat, ignition, and increasing ash residue percentage was shown in Fig. 6a. The first degradation stage was located between 85 and 115 °C, and then the main stage was started at 115 °C up to 308 °C, which describes the evaporation of CO and CO$_2$ by high percentages and 44.6% ash residue. It may return to break hemicelluloses and cellulose [34] as mentioned in Eq. (2) [12]:

$$2NaHCO_3(s) \rightarrow 2Na_2CO_3(s) + CO_2(g) + H_2O(g) \qquad (2)$$
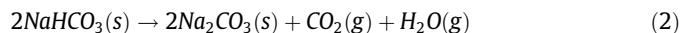
Synthesis of the new coating, including starch and p-Chloroaniline dimer (SK2) or aniline dimer (SK3), was mentioned in Fig. 6b. The presence of benzene ring in the structure of SK2 and SK3 specimens enhanced the thermal stability of the treated papers (SK2 and SK3) compared to untreated ones (SK0). Both of them record three stages of degradation different in ash residue since the SK3 specimen recorded ash residue percentage (31.2%) higher than SK2 (22.4%) and SK0 (1.3%) specimens.

In Fig. 6c, the SK6 specimen is higher than SK0 by 19.4%. In comparison, the presence of cellulose nanocrystalin the content of the coating leads toraising the ash residue of (SK8) to be the highest percentage (50.4%). This reversed in the p-chloroaniline dimer in Fig. 6d, since the SK9 specimen recorded a lower ash residue
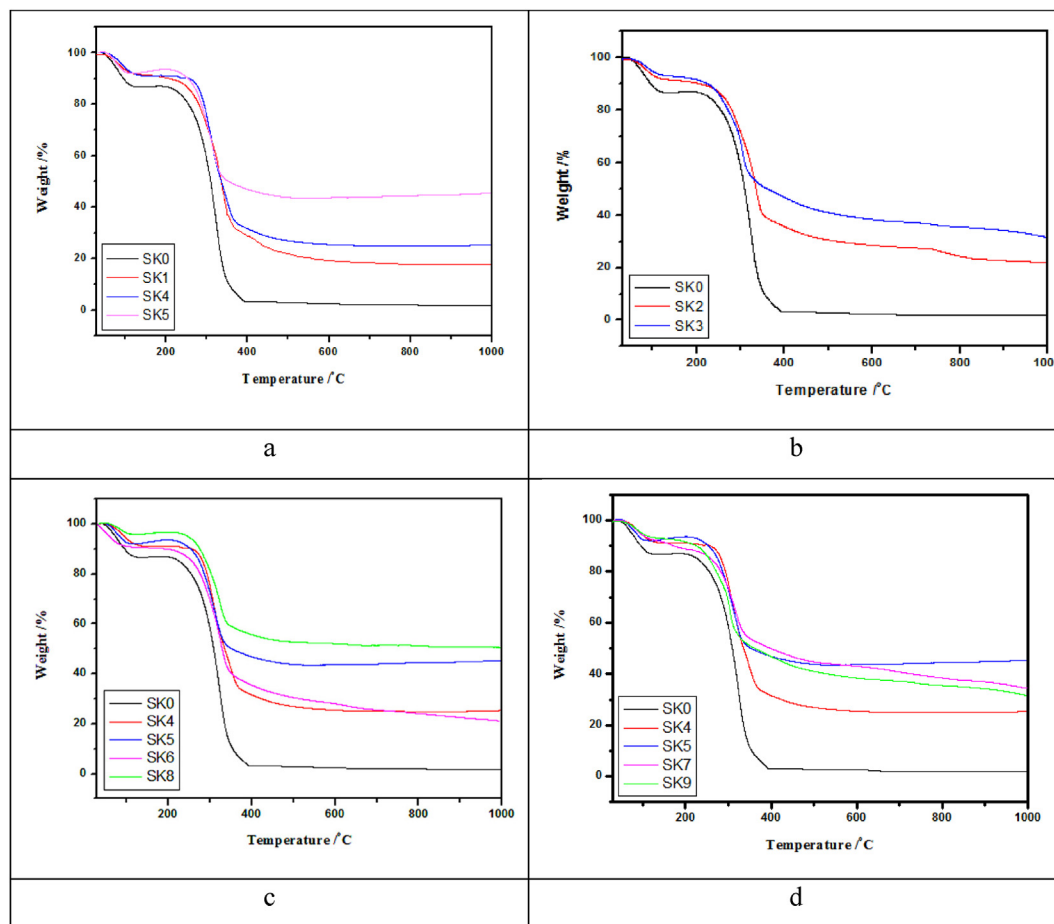

Fig. 6. Thermal analysis of SK0: Untreated bagasse paper, SK1: Specimen coated with 3.5% starch only, SK2: Specimen coated with 3.5% starch/0.50% p-chloroaniline dimer, SK3: Specimen coated with 3.5% starch/0.50% aniline dimer, SK4: Specimen coated with 5.0% starch only, SK5: Specimen coated with 5.0% starch/1.50%NaHCO$_3$/1.50%CaCO$_3$, SK6: Specimen coated with 5.0% starch/1.50%NaHCO$_3$/1.50%CaCO$_3$/0.50% aniline dimer, SK7: Specimen coated with 5.0% starch/1.50%NaHCO$_3$/1.50%CaCO$_3$/0.50% p-chloroaniline dimer, SK8: Specimen coated with 5.0% starch/1.50%NaHCO$_3$/1.50%CaCO$_3$/0.50% aniline dimer/10% CNCs, SK9: Specimen coated with 5.0% starch/1.50%NaHCO$_3$/1.50%CaCO$_3$/0.50% p-chloroaniline dimer /10% CNCs.
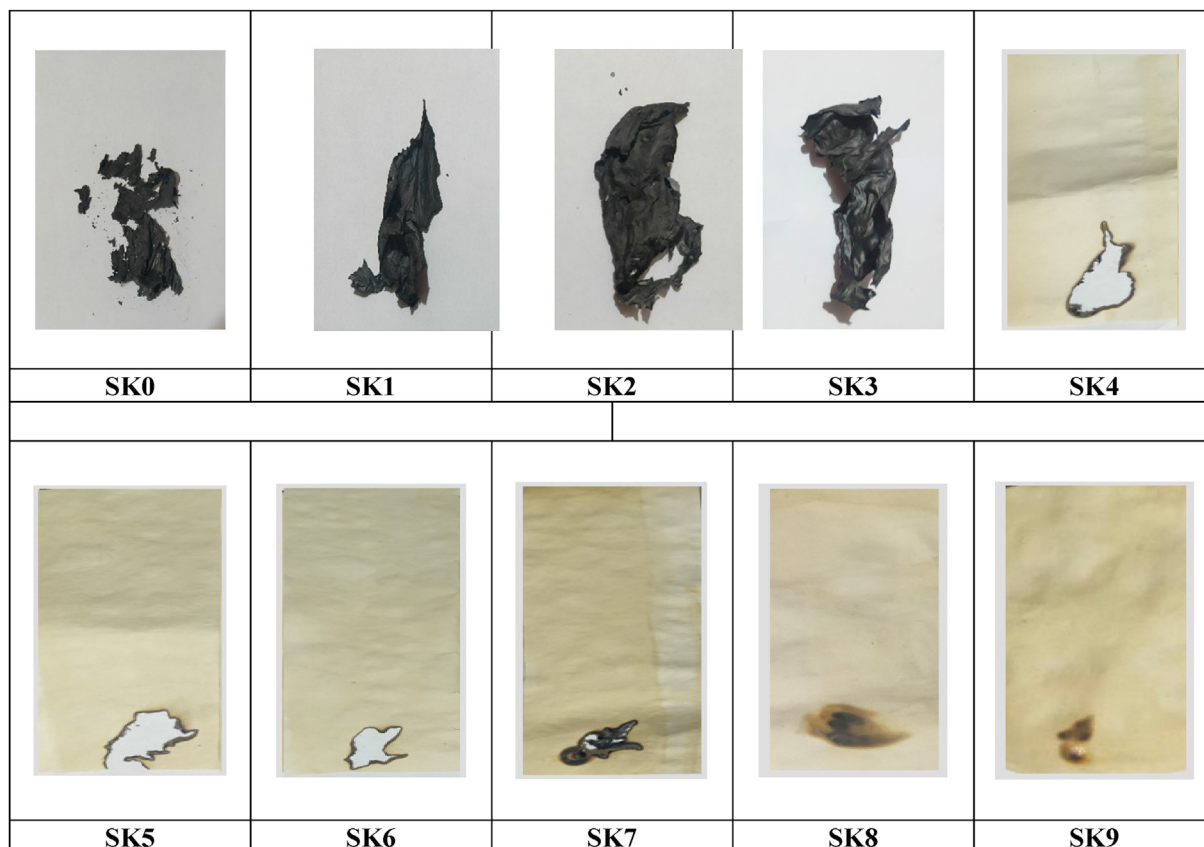
Fig. 7. Burning behavior test at ambient condition.

percentage (31.6%) compared to SK7 (34.3%). Both recorded enhancement in the thermal properties by 31.0% compared to SK0.

3.9. Flammability

Igniting the specimens in ambient condition explain the ability of SK4-9 specimens to fight ignition, as mentioned in Fig. 7. Complete burning with 13, 15, 25, and 38 s was recorded in the case of SK0-3, respectively. In comparison, the effect of starch after increasing the percentage to 5.0% was noticed in SK4 since the ignition stopped after 15sec. The presence of CO and CO_2 gases immersed from $NaHCO_3$ and $CaCO_3$ stopped the ignition from spreading in the up direction as noticed in SK5 specimen. The combustion area was decreased in the case of the SK6 specimen and stopped after 5sec. From this Figure, the combustion area and the ignition timedecrease by adding aniline dimer or p-

chloroaniline dimer, as noticed in SK6 and SK7 specimens, whereas cellulose nanocrystal has a direct effect at stop ignition in SK8-9 specimens.

The results of oxygen index and UL/94 were tabulated in Table 3. The lowest value of LOI was recorded for the SK0 specimen since it completely burnt at 19% with the highest burning rate (357.14 mm/min). In the case of the SK1 specimen, the oxygen percentage increased by 1.0%, and the burning time increased from 0.42% to 0.57%, with a burning rate of 263.17 mm/min due to the presence of starch. Enhancement is still achieved by the synthesis of a new coating using 3.5% of starch with 0.5% p-chloroaniline dimer (SK2) and 3.5% of starch with 0.5% aniline dimer (SK3). Due to complete burning all previous specimens had the same char length (15 cm).

The effect of starch percentage was noticed in the case of the SK4 specimen. It was burning in 21.8% of LOI with ash residue

Table 3
Oxygen index and burning rate of the untreated and treated specimens at ambient temperature.

Codes	LOI %	Δ LOI %	Burn length (mm)	Burning time (min)	Burning rate (mm/min)	Char length (cm)	Notes
SK0	19.0	0.0	150	0.42	357.14	15	Completely burnt with black smoke
SK1	20.0	1.0	150	0.57	263.17	15	Completely burnt with black smoke
SK2	20.1	1.1	150	0.62	241.94	15	Completely burnt with black smoke
SK3	20.8	1.8	150	0.75	200.0	15	Completely burnt with black smoke
SK4	21.8	2.8	0.0	0.0	0.0	2.0	Not burning
SK5	24.5	5.5	0.0	0.0	0.0	1.7	Not burning
SK6	26.3	7.3	0.0	0.0	0.0	1.2	Not burning
SK7	27.1	8.1	0.0	0.0	0.0	0.7	Not burning
SK8	27.5	8.5	0.0	0.0	0.0	0.8	Not burning
SK9	28.5	9.5	0.0	0.0	0.0	0.5	Not burning

All of these results are the average values of 5 reading within standard deviation ± 5%.

2 cm and self-extinguished in case of UL/94 when burning at ambient conditions. Due to the effect of starch molecules covering a high percentage of the specimen and obstructing oxygen from reacting with the specimen, this explains the effect of using different percentages of starch.

The cloud of gases such as CO and CO_2 was formed in the case of SK5-9 specimens due to cracking the $NaHCO_3$ and $CaCO_3$, as mentioned in Equation (1). The heightening started from SK6, which resists ignition up to 26.3%, and direct reaction with CNCs led to enhancing this resist up to 27.5% (SK8) without burning at ambient temperature. In the case of SK7 and SK9 specimens, the effect of p-chloroaniline dimer was noticed. Both resist fire up to 27.1 and 28.5%, respectively, with an enhancement of 8.1 and 9.5% compared to the untreated specimen (SK0).In the case of SK4-9, the char length varied from 1.7 cm up to 0.5 cm.

4. Conclusion

In this paper a new fire-resistant bagasse paper at a low cost based on the synthesis of 1,3-di-aryl-2,2,2,4,4,4-hexachlorocyclodi phosph(V)azane, where aryl is aniline or p-chloroaniline, were synthesized and reacted with cellulose nanocrystals to record high results compared to the untreated one. The physical and mechanical characteristics of the treated specimens were enhanced. Also, the thermal stability and ash residue is improved by increasing the starch, NaHCO3, CaCO3 and aryl-cyclodiphosph(V)azane percentage. Also, an enhancement in the resist fire compared to the untreated specimen, up to 27.5% with CNCs addition (SK8), without burning at ambient temperature was observed. According to the results, some additives may be produce a film on the top of the sheet after coating. These films decreasing the air permeability because they filled the pores and cover the surface by a coated thin layer. The best physical and mechanical characteristics of the treated specimens were recorded. The fire behaviour and combustibility of these treated papers were tested using LOI, and UL/94 recorded high values, which recorded enhancement compared to SK0 due to stopping fire breathing by decreasing oxygen gas percentage present in the fire tetrahedron. So, the treated bagasse paper can be used as an anti fire paper sheets of enhanced mechanical and physical properties desired as packaging materials.

Declaration of Competing Interest

The authors declare that they have no known competing financial interests or personal relationships that could have appeared to influence the work reported in this paper.

Acknowledgement

References

[1] S. Girish, K. Devendra, K.N. Bharath, Effect of sodium bicarbonate on fire behaviour of tilled E-glass reinforced epoxy composites, in: In: IOP Conference Series: Materials Science and Engineering. IOP Publishing, 2016, p. 012120.

[2] D. Bakirtzis, M.A. Delichatsios, S. Liodakis, W. Ahmed, Fire retardancy impact of sodium bicarbonate on ligno-cellulosic materials, Thermochim. Acta 486 (2009) 11–19.

[3] A.A. Younis, S.A.A. Mohamed, M.A. El-Samahy, A.H. Abdel Kader, Novel fire-retardant bagasse papers using talc/cyclodiphosphazane and nanocellulose as packaging materials, Egypt. J. Pet. 30 (2021) 25–32.

[4] S. Zhou, S. Li, X. Cao, Y. Qian, L. Li, X. Chen, Combustion behavior and thermal stability of ethylene-vinyl acetate composites based on $CaCO_3$ -containing oil sludge and carbon black, J. Therm. Anal. Calorim. 136 (2019) 1135–1145.

[5] V. Hernandez, R. Romero, S. Arias, D. Contreras, A novel method for calcium carbonate deposition in wood that increases carbon dioxide concentration and fire resistance, Coatings 12 (2022) 72.

[6] A. Strand, A. Khakalo, J. Kouko, A. Oksanen, A. Ketola, K. Salminen, A. Sundberg, The effect of chemical additives on the strength, stiffness and elongation potential of paper, Nord. Pulp Paper Res. J. 32 (2017) 324–335.

[7] M.M. Ibrahim, F. Mobarak, E.I.S. El-Din, A.E.H.E. Ebaid, M.A. Youssef, Modified Egyptian talc as internal sizing agent for papermaking, Carbohydr. Polym. 75 (2009) 130–134.

[8] Z. Yan, Q. Liu, Y. Deng, A. Ragauskas, Improvement of paper strength with starch modified clay, J. Appl. Polym. Sci. 97 (2005) 44–50.

[9] A.A. Ragheb, E.T.I. Abd, S. Tawfik, Gelatinization of starch in alkaline solutions, Starke 47 (1995) 338–345.

[10] W.J. Lim, Y.T. Liang, P.A. Seib, Cationic Oat Starch: Preparation and effect on paper strength, Cereal Chem. 69 (1992) 237–239.

[11] M.B. Ghazy, W.K. El-Zawawy, M.E. Owda, A.M. Elmeshtawy, Modified starch as additives to improve tissue paper properties, A. Az. B. Sci. 29 (2018) 55–70.

[12] A.A. Younis, S.A.A. Mohamed, M. El-Sakhawy, Fire resistant bagasse paper as packaging material using 1, 3-di-p-toluidine-2, 2, 2, 4, 4, 4-hexachlorocyclodiphosph (V) azane with hydroxyethyl cellulose, Egypt. J. Pet. 30 (2021) 29–36.

[13] A.C. Chapman, N.L. Paddock, Phosphonitrilic derivatives. Part VIII. The vibrational spectra of phosphonitrilic halides, J. Chem. Soc. 119 (1962) 635–645.

[14] M. El-Sakhawy, M.A. Nassar, H.M.F. Madkour, A.K. El-Ziatyand, S.A.A. Mohamed, Preparation and application of organophosphorus dimers as antimicrobial agent for bagasse packaging paper, Cellul. Chem. Technol. 52 (2018) 655–662.

[15] A.A. Younis, M.A. Nour, Kh. El-Nagar, Studying the effect of phosphorylated sol-gel on polyester fabric as flame-retardant coating, Elixir App. Chem. 70 (2014) 24230–24235.

[16] ISO 2759: Board. Determination of bursting strength, (2014).

[17] EN ISO 13934-1: Determination of maximum force and elongation at maximum force using the strip method, (2013).

[18] ASTM E1131: Standard test method for compositional analysis by thermogravimetry, (2020).

[19] A.A. Younis, Protection of polyester fabric from ignition by a new chemical modification method, J. Ind. Text. 47 (2017) 363–376.

[20] E. El-Alfy, F.A. Yassin, A.A. Younis, A.M. Salama, M. Hashem, Development of eco-friendly flame retardant finishing system for cotton fabrics, Macromole. An Indian J. 11 (2015) 14–23.

[21] BS 3119: Specification for method of test for flame proof materials (textile). British Standard Institution, London, (1959).

[22] A.A. Younis, Optimization of mechanical, thermal and ignition properties of polyester fabric using urea and phosphoric acid, J. Ind. Text. 49 (2020) 791–808.

[23] A.A. Younis, Evaluation of the flammability and thermal properties of a new flame retardant coating applied on polyester fabric, Egypt. J. Pet. 25 (2016) 161–169.

[24] A.A. Younis, Evaluation flammability, mechanical and electrical properties of polypropylene after using zinc borates and montmorillonite, J. Thermoplast. Compos. Mater. 35 (2022) 177–191.

[25] A.A. Younis, Kh. El-Nagar, M.A. Nour, Part I: Characterization of flammability behavior of polyester fabric modified with sol-gel, Int. J. Chem. 5 (2013) 38–42.

[26] M.A. Razali, A. Sapit, A.N. Mohammad, H. Salleh, R.H. Madon, Effect of baggase physical properties and composition on flame spread behavior, Int. J. Integr. Eng. 12 (2020) 271–277.

[27] ISO 4589-2: Plastics — Determination of burning behaviour by oxygen index — Part 2: Ambient-temperature test, (2017).

[28] A.A. Younis, Flammability properties of polypropylene containing montmorillonite and some of silicon compounds, Egypt. J. Pet. 26 (2017) 1–7.

[29] E.A. El-Alfy, A.A. Younis, S.H. Samaha, A.M. Salama, Eco –friendly flame retardant via self assembly coating, Egypt. J. Chem. 60 (2017) 479–489.

[30] A.A. Younis, Flame retardancy, mechanical properties and antibacterial activity for polyester fabric coated with a sol-gel coating and pomegranate rind, Fibers Polym. 20 (2019) 2594–2603.

[31] S.A.A. Mohamed, M. El-Sakhawy, S. Kamel, Water resistance and antimicrobial improvement of bagasse paper sheet by microwave modification with fatty acid and Ag-NPs nanocomposite, Cellul. Chem. Technol. 52 (2018) 423–431.

[32] Y. Ding, B. Huang, K. Li, W. Du, K. Lu, Y. Zhang, Thermal interaction analysis of isolated hemicellulose and cellulose by kinetic parameters during biomass pyrolysis, Energy 195 (2020) 117010.

[33] J.J. Chew, M. Soh, J. Sunarso, S.T. Yong, V. Doshi, S. Bhattacharya, Gasification of torrefied oil palm biomass in a fixed-bed reactor: effects of gasifying agents on product characteristics, J. Energy Inst. 93 (2020) 711–722.

[34] S.A.A. Mohamed, M. Sc, Thesis, Faculty of Science, Al-Azhar University, Cairo, (2006).